Silver Nano-Particles from Diesel Particulate Matter: An Environmental Pollutant to a Potential Antimicrobial Agent and a Photocatalyst

7 authors, including:

L. Palliyaguru
University of Sri Jayewardenepura
13 PUBLICATIONS   **30** CITATIONS

SEE PROFILE

Neluka Fernando
University of Sri Jayewardenepura
139 PUBLICATIONS   **979** CITATIONS

SEE PROFILE

Chinthika Gunasekara
University of Sri Jayewardenepura
104 PUBLICATIONS   **719** CITATIONS

SEE PROFILE

Champa Disala Jayaweera
University of Sri Jayewardenepura
38 PUBLICATIONS   **100** CITATIONS

SEE PROFILE

Some of the authors of this publication are also working on these related projects:

ilmenite View project

Removal of metals and hazardous dyes from wastewater by low cost materials View project

Silver Nano-Particles from Diesel Particulate Matter: An Environmental Pollutant to a Potential Antimicrobial Agent and a Photocatalyst

L. Palliyaguru[a], M.U.S. Kulatunga[a], K.G.U.R. Kumarasinghe[a], S.S.N. Fernando[b], T.D.C.P. Gunasekara[b], C.D. Jayaweera[a], P.M. Jayaweera[a,*]

[a] Dept. of Chemistry, University of Sri Jayewardenepura, Nugegoda, Sri Lanka

[b] Dept. of Microbiology, University of Sri Jayewardenepura, Nugegoda, Sri Lanka

Abstract- The water soluble fraction (WSF) of diesel particulate matter (DPM), an environmental pollutant was used to synthesize silver nanoparticles (AgNPs). FTIR, fluorescence and UV-Vis data suggest that water soluble oxygenated PAHs in the WSF of DPM are capped to the surface of AgNPs providing the stability. The particle size, the size distribution, and the crystalline nature were confirmed by transmission electron microscopy (TEM) and X-ray diffraction (XRD) analysis. The particles are spherical in shape having an average size of 7.7±1.5 nm. The antimicrobial activity of synthesized AgNPs was investigated using Agar well diffusion method and an enhanced activity was shown against the pathogens of *Candida albicans*, *Escherichia coli* and *Staphylococcus auerus*. A high level of photocatalytic activity for the degradation of rhodamine B and 2,4-dichlorophenoxyacetic acid (2,4-D), a common dye and a pesticide was exhibited by the AgNPs.

Keywords- Ag nanoparticles, Diesel particulate matter, Antimicrobial activity, Photocatalyst

I. INTRODUCTION

Diesel particulate matter (DPM) arising from diesel combustion has a number of undesirable environmental impacts on human health, climate, and ecology [1, 2]. Both stationary and mobile applications based on diesel combustion are heavily used throughout the world such as in electric power plants and automobile industry. Although, diesel particulate filters are installed in engines to reduce the emission of particulates to the environment, a large amount of DPM is discharged to the environment, especially during the regeneration process of the particulate filters [3]. Hence, the ability to utilize DPM for a potential application can be highly beneficial to the environment [4, 5].

DPM contains carbonaceous materials that includes unburned fuel molecules, partially burned fuel molecules, inorganic matter, and oxygenated PAHs adsorbed onto elemental carbon [6, 7]. Oxygen inside the internal combustion engine reacts with the hydrocarbons present in diesel fuel to produce a broad range of compounds that include aliphatic and aromatic aldehydes, mono- and poly- substituted benzene, and oxygenated PAHs [8-10]. The polarity of these organic compounds varies widely and some of which are water soluble [11, 12].

Among many types of metallic nanoparticles, AgNPs have shown a broad range of applications in medicine, renewable energies, and environmental remediation due to their unique optical, electrical, thermal and biological properties [13-17]. Controlling the physicochemical properties of AgNPs is a key aspect in developing technological applications which is heavily dependent on the method of synthesis, temperature, nature of the reducing and stabilizing agents. The chemical methods [14, 15, 18] hold several advantages over the other preparation methods, such as the simplicity in the procedure, and the consistency in the physicochemical properties. In chemical methods, the preparation of colloidal dispersion of AgNPs in water or in organic solvents is generally performed by chemical reduction. The use of naturally occurring reducing agents such as polysaccharides, plant extracts, or liquid mixtures of microorganisms has become popular in the synthesis of AgNPs due to the low cost and minor environmental impact [19-21]. Plant extracts, generally contain fairly large number of carbonyl and phenolic compounds that collectively provide a sufficient potential for the reduction of silver ions to metallic silver and the required stability for the AgNPs [22]. The aggregation of metallic silver atoms in to nano-sized, usually spherical particles are subsequently stabilized either by electrostatic or steric forces [23-25].

One of the most noticeable characteristics of AgNPs is its antimicrobial property. Silver is well known for its inhibitory effect on many microorganisms commonly present in medical and industrial processes [26]. Antimicrobial property of silver is greatly enhanced, if silver is transformed to a nanoparticle. This paper reports the antimicrobial potential of synthesized AgNPs against three common pathogens, *Candida albicans*, *Escherichia coli* and *Staphylococcus auerus*. Furthermore, the photocatalytic activity of AgNPs has gained a renewed interest in redox conversions of some organic compounds [27-30]. Silver nano particles give rise to SPR, which results from oscillating electrons of silver under the influence of visible light in the wavelength ranging

from 400 - 500 nm. This unique behaviour is limited to a few metals like Au, Ag, Cu, and Pt [27]. Exploiting this property is already seen in many applications that include surface-enhanced Raman spectroscopy, photocatalysis and in biosensors [31, 32]. We have successfully used the AgNPs synthesized from WSF of DPM for the photocatalytic degradation of an organic dye, rhodamine B and a pesticide, 2,4-D. In the present study, fluorescence quenching behavior of oxygenated PAHs and the surface plasmon resonance (SPR) peak intensities were analyzed as a function of WSF of DPM to Ag ion concentration to determine the capping action of the oxygenated PAHs in the formation of AgNPs. The idea of using DPM in the synthesis of AgNPs is novel and has not been previously attempted to our knowledge and we have proved the possibility of synthesizing AgNPs directly from the diesel engine exhaust.

II. MATERIALS AND METHODS

A. Preparation of the water extract of DPM

DPM was collected from diesel particulate filters located near the engines of passenger transport vehicles of a central depot in Colombo, Sri Lanka. A Soxhlet extraction method was used to obtain the water soluble fraction of DPM. A volume of 200 mL of double distilled, deionized water and 2.0 g of DPM were used for the extraction. The Soxhlet apparatus was adjusted to 8 cycles per hour and was run continuously for 8 hours.

B. Synthesis of AgNPs from DPM

Firstly, 8.0 mL of fresh water extract of DPM and 2.0 mL of 0.2 M KOH (Loba Chemie) were mixed to make the water extract basic. Then, 7.5 mL of the basified extract was gradually introduced to a boiling solution of 140 mL of 1.0 mM $AgNO_3$ (Park Scientific) under constant stirring within a period of 30 minutes. The solution was continually heated and stirred for another 30 minutes. The solution was cooled down prior to the use.

C. Synthesis of AgNPs from direct diesel engine exhaust (DEE)

A direct injection, light duty Toyota 2C diesel engine was run on the idle mode to produce continuous and uniform flow of exhaust fume. The exhaust pipe was directly connected to a three-neck round-bottom flask containing a volume of 200 mL of distilled water adjusted to pH 9 with KOH. The diesel engine exhaust was purged into the three-neck round-bottom flask for 30 minutes. Then, 5 mL of this solution was gradually added to a boiling solution of 100 mL of 1.0 mM $AgNO_3$ under constant stirring within a period of 30 minutes. The solution was allowed to cool prior to the use.

D. Characterization of AgNPs

The preliminary characterization of synthesized AgNPs was carried out using a Perkin Elmer Lambda 35 UV-Vis spectrometer. The morphology of AgNPs was assessed by the high resolution transmission electron microscopy (HR-TEM ZEISS Libra 200 Cs-TEM) at an accelerating voltage of 200 kV. The X-ray diffraction pattern of synthesized AgNPs were obtained using Ragaku Ultima-IV diffractometer. The Fourier Transform Infrared spectroscopy, FTIR (Thermo Scientific Nicolet iS10) spectra were recorded using KBr pellets. Powdered samples were obtained by centrifugation at 40,000 rpm (SORVALL RC M120GX) for ~20 minutes.

E. Fluorescence quenching of PAHs by AgNPs

Fluorescence spectra were obtained (Thermo Scientific Lumina) for a series of samples prepared by varying volume ratios (0:10 – 10:0) of 1.0 mM Ag^+ : WSF of DPM (pH of 12). For all fluorescence measurements, the excitation wavelength was set at 350 nm and emission spectra were recorded in the wavelength range of 380 nm to 600 nm. UV-Vis spectra of each mixture were also recorded in order to detect AgNPs formation via the SPR peak. Crystals of NaCl were added and fluorescence intensity was re-measured at room temperature of the samples that showed a drop in the fluorescence intensity after the addition of silver ions into the WSF of DPM.

F. Microorganisms

Candida albicans (ATCC 10231), *Escherichia coli* (ATCC 25922) and *Staphylococcus aureus* (ATCC 25623) were obtained from the culture collection (Department of Microbiology, Faculty of Medical Sciences, University of Sri Jayewardenepura). *Candida albicans* was cultured in Sabouraud Dextrose Agar (HiMedia) and *Escherichia coli* and *Staphylococcus aureus* were cultured in nutrient agar (HiMedia) for 18 hours at 37 °C before each experiment.

G. Antimicrobial activity by agar well diffusion assay

Antimicrobial activity of the synthesized AgNPs was determined using the well diffusion method [33]. Overnight grown cultures of the test organisms were suspended in sterile physiological saline and the absorbance was adjusted to 0.5 McFarland standard. The standard bacteria suspension and *Candida* suspension were lawned on Mueller Hinton Agar (MHA, HiMedia, India) and SDA (HiMedia, India), respectively using the spread plate method. A sterile 9 mm cork borer was used to prepare wells and the bottoms of the wells were sealed with sterile molten agar. The wells were loaded with 200 µl of freshly prepared AgNPs solutions from both WSF of DPM and the direct DEE. The three control wells were loaded with 1mM $AgNO_3$, sterile distilled

water and the water extract of DPM. Plates were incubated at 37 °C for 24 hours. All experiments were done in triplicates. The average Zone of inhibition (ZOI) was calculated.

H. Photocatalytic study

The photocatalytic experiments using the synthesized AgNPs were carried out for an organic dye, rhodamine B (Loba Chemie) and a common pesticide, 2,4-D (Sigma-Aldrich). The test solutions containing 100.0 mL of distilled water and 100 μl of AgNPs were mixed with either rhodamine B or 2,4-D until an optical absorbance of one at its maximum absorbance wavelength was reached. The samples were irradiated using a Philips Hg arc 250 W UV-Vis light source. The rate of photodegradation was studied by measuring the absorbance at 550 nm (for Rhodamine B), and 283 nm (for 2,4-D) of the test solutions by withdrawing samples at 0, 30, 60 and 90, 120, and 150 minutes illumination time intervals. Control experiments were also carried out with 100.0 mL of water and 50.0 mL of the analyte in the absence of AgNPs. The test solutions were kept under dark conditions for 30 minutes to equilibrate before irradiation.

III. RESULTS AND DISCUSSION

A. Nanoparticle characterization

The synthesised AgNPs produce a characteristic absorption in the UV-Vis spectrum (Figure 1b) around 400-500 nm region due to the surface Plasmon resonance (SPR). The appearance of a peak at 401 nm, with a FWHM (Full Width at Half Maximum) of 80 nm is a strong indication for the formation of AgNPs with smaller particle sizes. The WSF of DPM does not show any absorption features in the 400 nm region (Figure 1a).
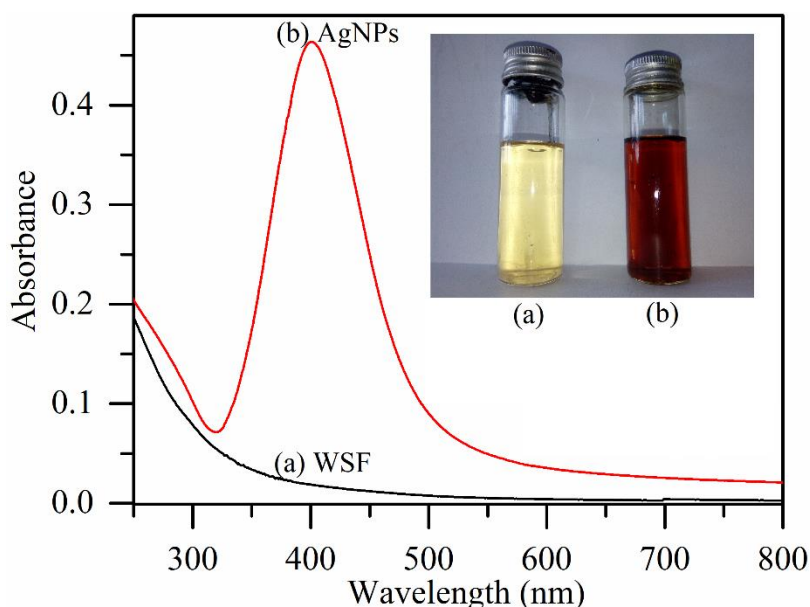

Figure 1: UV-Vis absorption spectra of (a) WSF of DPM and (b) synthesized AgNPs from WSF.

The surface morphology of the synthesized AgNPs was studied by TEM images. The TEM image (Figure 2.) indicates that AgNPs are spherical in shape and are fairly monodispersed. The inset of Figure 2 shows the particle size distribution of AgNPs derived from TEM data. The average diameter of the nanoparticles is 7.7±1.5 nm, which is smaller than the average diameters of AgNPs synthesized from some reported plant extracts [21, 34]. Having a smaller particle size is advantageous to enhance the properties like photocatalytic and antimicrobial activities.
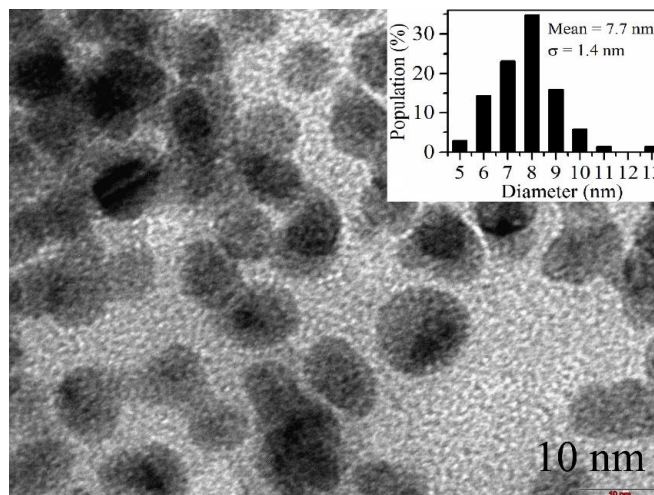
Figure 2: TEM image of synthesized AgNPs. Insert: Particle size distribution.

X-ray diffraction pattern recorded for the synthesized AgNPs (Figure 3) is matched with the peak distribution of metallic silver (Ag, JCPDS # 89-3722). The four peaks of pure silver observed at 2θ = 38.09°, 44.30°, 64.43° and 77.42° in the diffractogram are index as (1 1 1), (2 0 0), (2 2 0), and (3 1 1), respectively. The crystal nature of synthesized AgNPs is particularly evident by the XRD data. The UV-Vis, TEM, and XRD data collectively provide a strong evidence for the formation of AgNPs from the molecules present in the WSF of DPM.
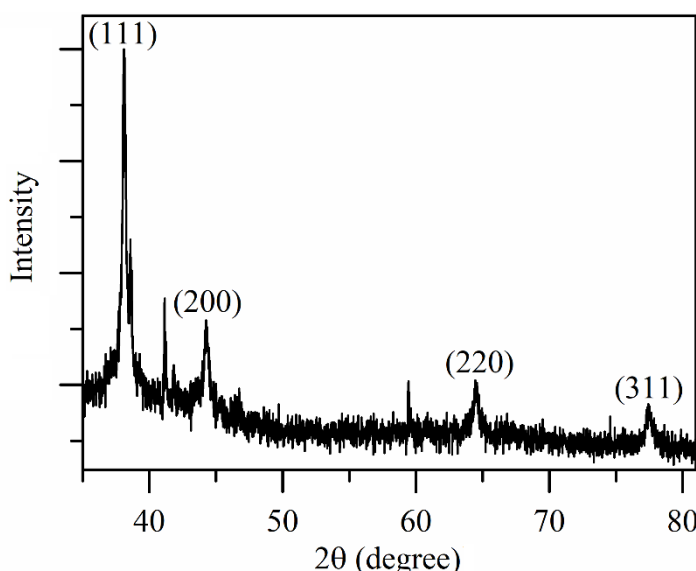

Figure 3: X-ray diffraction pattern of synthesized AgNPs.

The chemical nature of organic compounds present in the WSF of DPM plays a vital role in understanding the mechanism behind the formation of AgNPs. The FTIR spectra of DPM, WSF of DPM and the synthesized AgNPs are shown in Fig. 4. The FTIR spectrum of DPM (Figure 4a), clearly shows the vibration modes corresponding to the hydroxyl (~3442 cm^{-1}), and carbonyl (~1602 cm^{-1} and 1718 cm^{-1}) groups. The appearance of a weak peak at 2921 cm^{-1} corresponds to the aliphatic C-H stretching vibration modes. Figure 4a is in strong agreement with the previously recorded FTIR spectrum of DPM [35]. As reported in previous investigations [8, 11], DPM contains a variety of compounds from oxygenated PAHs, mono and poly-substituted benzenes, to aliphatic aldehydes, and ketones corresponding to a broad range of polarities. According to Liang et al.[6], 20-percent of the total organic compounds in diesel soot corresponds to n-alkanoic and aromatic acids. The low pH (2.7) of the WSF of DPM, further indicates the presence of a significant amount of carboxylic acids in WSF of DPM. The FTIR spectrum of a freeze dried sample of WSF of DPM (Figure 4b) confirms the presence of organic compounds in the water extract of DPM. The peaks around 3400 cm^{-1} and 1718 cm^{-1} correspond to the presence of hydroxyl and carbonyl compounds. The presence of a broad peak at 3350 cm^{-1} and a sharp peak at 1636 cm^{-1} in the FTIR spectrum of AgNPs (Figure 4c) synthesized from WSF of DPM is a direct confirmation for the involvement of hydroxyl/oxo substituted organic compounds during the formation of AgNPs. Peaks at 1046 cm^{-1} can be assigned to –C–O (ether linkages) [36] and the peak at 1402 cm^{-1} may be assigned to geminal methyls based on the previously published work [37]. The bands at 3350 cm^{-1} correspond to -OH stretching vibrations indicating the

presence of alcohol and/or phenol [38]. The studies based on aqueous extracts of plant materials to synthesize AgNPs have shown a strong connection between the presence of organic compounds with a minimum of two hydroxyl groups at *ortho* and *para* positions of a phenyl ring and a tendency to reduce and stabilize the silver ions to its metallic form [39]. Therefore, the hydroxyl compounds in the WSF of DPM as confirmed by the FTIR analysis play a similar role during the formation of AgNPs.
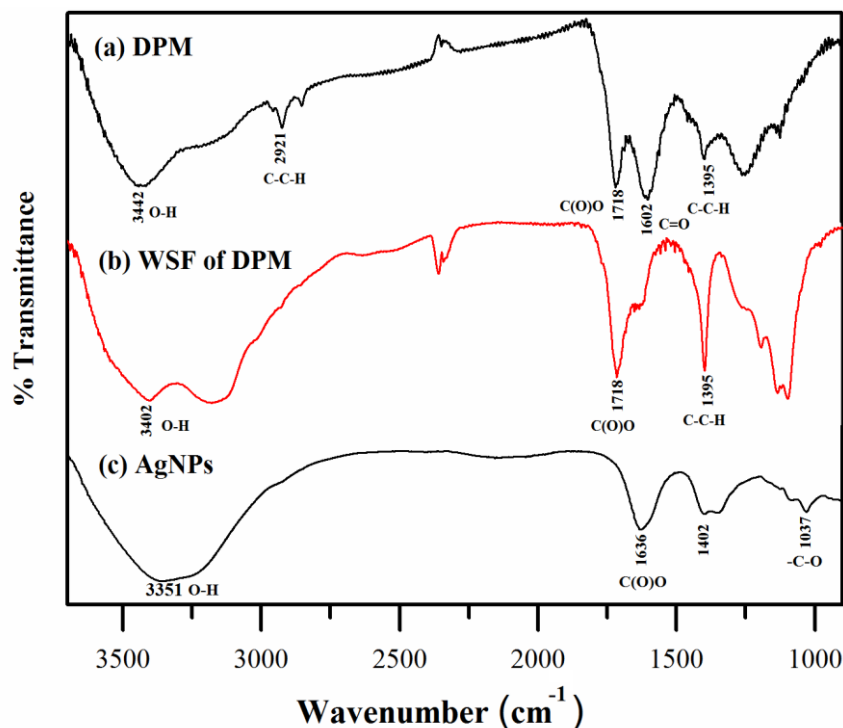
Figure 4: FTIR spectra of (a) DPM, (b) WSF of DPM and (c) synthesized AgNPs from WSF.

B. AgNPs from diesel engine exhaust fumes

The UV-Vis absorption spectrum of AgNPs synthesized directly from the diesel engine exhaust fumes (DEEF) is shown in Figure 5. The SPR peak is positioned at 409 nm and has a FWHM of 160 nm, which is broader than the FWHM of the SPR peak observed for the AgNPs synthesized from the WSF of DPM. It indicates a broader particle size distribution for the AgNPs synthesized from direct DEEF when compared with WSF of DPM. The inset in Figure 5 is the XRD pattern of the AgNPs synthesized from direct DEEF. The DEEF contains a large amount of volatile organic compounds in addition to diesel particulate matter [40]. Therefore, a wider range of reducing agents could be available to form the AgNPs during the synthesis than from the WSF of DPM. This confirms that the synthesis of AgNPs by DEEF is simple and faster than extracting WSF from DPM.
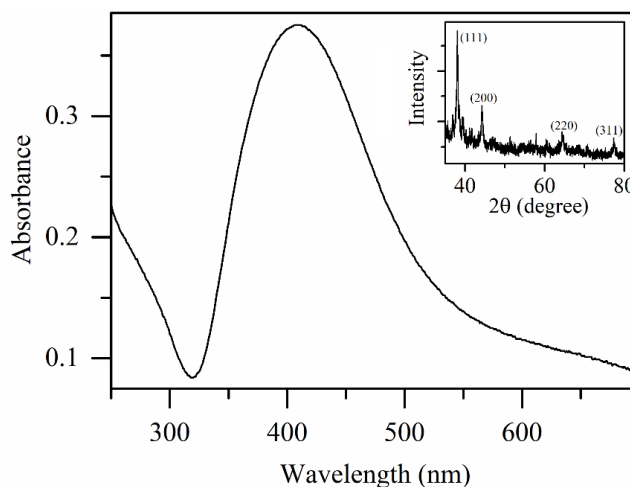
Figure 5: UV-Vis absorption spectrum of AgNPs synthesized directly from the DEEF. Inserted: X-ray

diffraction pattern.

C. The role of oxygenated PAHs in the formation of AgNPs

The intense fluorescence signal observed at 420 nm for WSF of DPM allows to understand the capping action of water soluble PAHs. In this regard fluorescence quenching studies (*see* Figure 6a) were performed with the addition of varying volume ratios of Ag^+ to the WSF of DPM. A gradual decrease in the fluorescence signal was observed as a function of increasing Ag^+ concentration for the mixtures up to 0 % to 40%. A sudden drop in the fluorescence signal was observed after mixtures having >50% of Ag ions. UV-Vis absorption spectra were also recorded simultaneously for the same samples (*see* Figure 6c) and the appearance of SPR peak at 470 nm was evident at a ratio of 1:1 with a drop in the fluorescence intensity suggesting the surface capping of fluorophores present in the WSF to the AgNPs. In order to confirm that the observed drop in the fluorescence signal was not due to the dilution effect, a control experiment (*see* Figure 6b) replacing Ag^+ with water was also carried out.
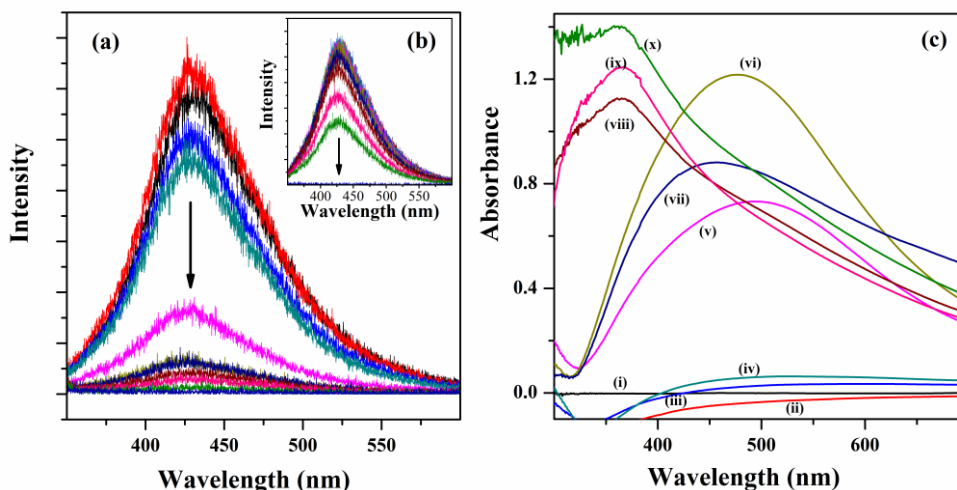

Figure 6: Fluorescence emission spectra for the mixtures containing different volume ratios (a) WSF and Ag^+ (10:0 to 0:10). (b) WSF and H_2O (10:0 to 0:10). (c) UV-Vis absorption spectra for the mixtures containing different volume ratios WSF and Ag^+ (10:0 to 0:10) represented by (i)-(x).

The relative fluorescence intensities (i.e. I/I_0 at max.) *vs.* ratios of Ag^+ to the WSF of DPM were plotted (Figure 7a). It shows a sharp drop after 40% of Ag^+ addition into the WSF of DPM, indicating the presence of an efficient fluorescence quenching process, occurring once AgNPs are formed. Whereas, addition of water, i.e. control experiment (*see* Figure 7b) suggests that the decrease in the fluorescence intensity is due to the dilution effect. The quenching of fluorescence of oxygenated PAHs by AgNPs may arise from the formation of a static complex via electrostatic interactions. A previous investigation[16] using fluorescing molecules as a local probe of the surface Plasmon field of metallic NPs, indicated that the quenching rate showed a strong correlation on the distance between the probe and the metal surface. A direct binding of the fluorescing probe to the metal surface resulted a complete quenching.
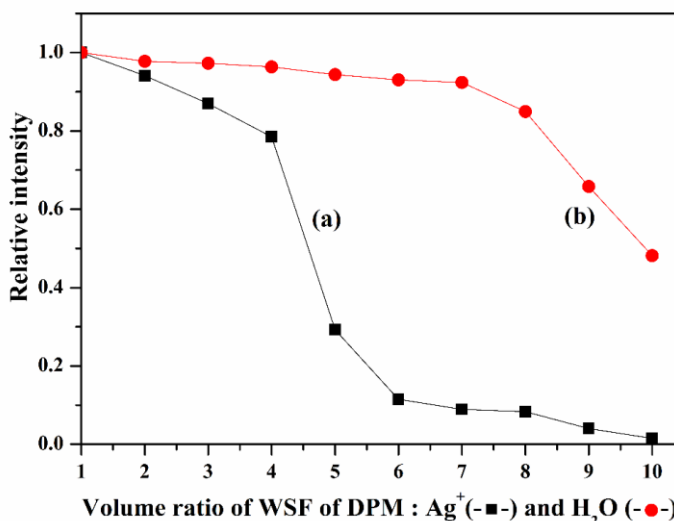

Figure 7: The variation of fluorescence emission intensity as a function of volume ratio between WSF of DPM and (a) Ag^+ (b) H_2O.

Figure 8(a) demonstrates the recovery of fluorescence signal from synthesized AgNPs samples by changing the ionic strength with the addition of NaCl. The formation of an electrostatic complex during the quenching process was further supported by the recovery of the fluorescence signal upon changing the ionic strength [41]. A sample of synthesized AgNPs displaying quenched fluorescence (Fig. 8a(i)) was mixed with a few NaCl crystals at room temperature to recover the signal as shown in Figure 8a(ii). Figure 8(b) shows the UV-Vis absorption spectra of the samples used to obtain the data in Figure 8a(i) and Figure 8a(ii). The sample with recovered fluorescence signal has no SPR peak (Figure 8b(ii)) indicating a dissociation of electrostatic complex/AgNPs to release oxygenated PAHs to fluoresce. Therefore, it can be concluded that oxygenated PAHs in WSF of DPM act as capping materials in the synthesis contributing to the stability of AgNPs.
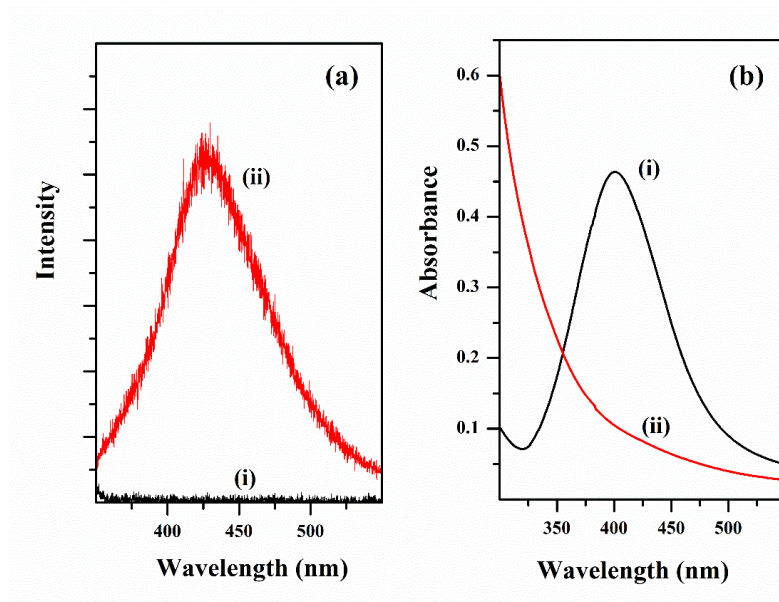

Figure 8: (a) The florescence emission spectra of (i) before (ii) after addition of NaCl. (b) UV-Vis absorption spectra of (i) before addition of NaCl. (ii) after addition of NaCl for the synthesized AgNPs from WSF.

D. Antimicrobial activity

The presence of a zone of inhibition (ZOI) for the two types of AgNPs synthesized through WSF of DPM and direct DEEF demonstrated antimicrobial activity against *C. albicans*, *E. coli* and *S. aureus* (*see* Table I). The antimicrobial activity of the AgNPs was compared with 1 mM $AgNO_3$ solution. Sterile distilled water and water extract of DPM were used as the negative control. All tested microorganisms exhibited comparable ZOIs to 1 mM $AgNO_3$, which is a well-known antimicrobial agent (Figure 9). AgNPs synthesized with the WSF of DPM exhibited a stronger antimicrobial activity compared to DEEF AgNPs (Figure 9 and Table I). The yeast *C. albicans* exhibited the strongest inhibition by both types of AgNPs compared to the bacteria *E.coli* and *S. aureus.* The water extract of DPM do not show any ZOI for all three microorganisms, indicating an insignificant level of antimicrobial activity. The results clearly indicate that AgNPs synthesized and stabilized with water soluble compounds present in the DPM is a potent antimicrobial agent against the investigated microbes.
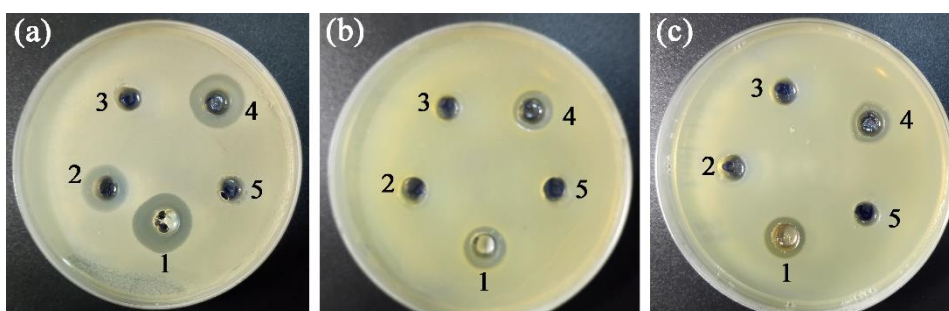

Figure 9: Antimicrobial activity determined using agar well diffusion method. Photograph of (a) C. albicans, (b) E. coli and (c) S. aureus. ZOI of 1, 2, 3, 4 and 5 are for $AgNO_3$, direct DEE-AgNPs, WSF of DPM, WSF-AgNPs and distilled water (DW), respectively.

Table I. Average zones of inhibition of the AgNPs against the three test organisms after incubation at 37 °C for 24 hrs. ZOI of 1, 2, 3, 4 and 5 are for AgNO₃, direct DEE-AgNPs, WSF of DPM, WSF-AgNPs and distilled water (DW), respectively.

Organism	ZOI (mm)				
	AgNO$_3$	Direct DEE-AgNPs	WSF of DPM	WSF-AgNPs	DW
Candida albicans	1.8 ± 0.07	1.4 ± 0.07	-	1.6 ± 0.14	-
Escherichia coli	1.2 ± 0.07	1.0 ± 0.07	-	1.2 ± 0.12	-
Staphylococcus auerus	1.2 ± 0.07	1.0 ± 0.07	-	1.1 ± 0.07	-

A high surface to volume ratio of smaller AgNPs results in higher antimicrobial potential. It has been reported that AgNPs bind to the surface of the cell membrane thereby disrupting its functions [42]. Silver ions released from the cell membrane contribute to the antimicrobial activity [43]. Further, the NPs penetrate the cell membrane and bind to intracellular organelles such as the mitochondria and nucleus leading to disruption of metabolic pathways and DNA replication [44]. The structure, thickness and composition of the cell wall are important factors affecting the antimicrobial activity. The Gram positive cell wall of *S. aureus* has greater cell wall thickness compared to Gram negative bacteria. Further the negatively charged cell wall peptidoglycan results in the Ag ions being stuck on to the cell wall preventing the penetration inside the cell and whereby Gram positive bacteria become more resilient to its action. In contrast, the thin cell wall of Gram negative bacteria containing Lipopolysaccharides which have a high negative charge promotes adhesion of AgNPs and its penetration within the cell [45]. Further the strong antimicrobial activity of AgNPs observed in this study against *Candida albicans* is suggested to be due to the NPs acting on yeast cells by disrupting the cell membrane and inhibiting the normal budding process due to its negative impact on membrane integrity [46].

3.5 Photocatalytic activity of synthesized AgNPs

The surface Plasmon induced photocatalytic activity of AgNPs prepared by the WSF of DPM was assessed using the photodegradation of an organic dye, rhodamine B, and a widely used pesticide 2,4-D (2,4-Dichlorophenoxyacetic acid). The photodegradation was measured by monitoring the absorbance at the maximum absorption wavelength, 560 nm for rhodamine B and 290 nm for 2,4-D. The degradation kinetics are shown in Figure 10a and 10b. The analyte samples exhibit a significant level of photodegradation in the presence of AgNPs.
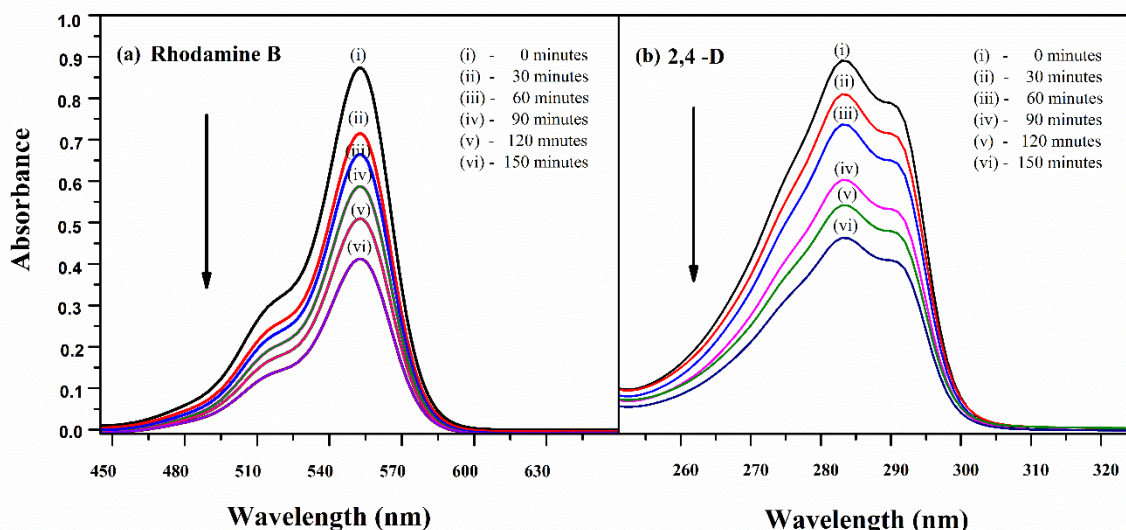

Figure 10: The photodegradation of (a) rhodamine B and (b) 2,4-dichlorophenoxyacetic acid in the presence of AgNPs as a function of irradiation time.

The drop of the analyte concentration after 150 minutes of exposure to the UV-Vis radiation was 41-percent for rhodamine B and 39-percent for 2,4-D, in the presence of the same catalytic load. The control experiments were also carried out in the absence of AgNPs for the samples and showed only about 3-percent of photodegradation within the same exposure time (not shown in the figure). The fast degradation of the analyte molecules under UV-Vis light irradiation in the presence of AgNPs suggests that the catalytic reaction is greatly accelerated by UV-Vis radiation. AgNPs absorb UV-Vis photons due to interband electron transitions and localized surface Plasmon resonance effect. The mechanism of the Plasmon-induced reaction can be represented in the following manner [47];

$$Ag + h\nu \rightarrow e^{-} + h^{+} \tag{1}$$

$$e^{-} + O_2 \rightarrow \bullet O_2^{-} \tag{2}$$

$$\bullet O_2^{-} + H_2O \rightarrow OH^{-} + \bullet HO_2 \tag{3}$$

$$\bullet HO_2 + \bullet HO_2 \rightarrow H_2O_2 + O_2 \tag{4}$$

$$H_2O_2 + \bullet O_2^{-} \rightarrow \bullet OH + OH^{-} + O_2 \tag{5}$$

$$H_2O + h^{+} \rightarrow \bullet OH + H^{+} \tag{6}$$

$$dye + \bullet O_2^{-} \text{ (or } \bullet OH, H_2O_2) \rightarrow degradation\ products \tag{7}$$

IV. CONCLUSIONS

The water soluble fraction (WSF) of DPM, a known environmental pollutant was utilized as a novel reducing agent for the synthesis of AgNPs. The method is simple when compared with the existing methods. TEM confirms that the synthesized AgNPs are spherical in shape with an average diameter of 7.7 nm. Further, the synthesis of AgNPs from diesel engine exhaust fumes (DEEF) is possible and the present study has revealed that the water soluble organic compounds formed during the internal combustion of diesel fuel can convert silver ions in to silver nano-clusters under basic conditions. The AgNPs synthesized either by WSF of DPM or the DEEF display the potential antimicrobial activity against *Candida albicans*, *Escherichia coli* and *Staphylococcus auerus.* The surface Plasmon induced photocatalytic activities were also observed for the organic dye, rhodamine B and a common pesticide 2,4-D.

ACKNOWLEDGEMENTS

REFERENCES

[1] C. I. Davidson, R. F. Phalen, and P. A. Solomon, "Airborne Particulate Matter and Human Health: A Review," *Aerosol Science and Technology,* vol. 39, no. 8, pp. 737-749, 2005.

[2] J. Liu, X. Q. Ye, D. P. Ji, X. F. Zhou, C. Qiu, W. P. Liu*, et al.*, "Diesel exhaust inhalation exposure induces pulmonary arterial hypertension in mice," *Environmental Pollution,* vol. 237, pp. 747-755, 2018.

[3] B. A. A. L. van Setten, M. Makkee, and J. A. Moulijn, "Science and technology of catalytic diesel particulate filters," *Catalysis Reviews,* vol. 43, no. 4, pp. 489-564, 2001.

[4] A. Singh, P. Khare, S. Verma, A. Bhati, A. K. Sonker, K. M. Tripathi*, et al.*, "Pollutant Soot for Pollutant Dye Degradation: Soluble Graphene Nanosheets for Visible Light Induced Photodegradation of Methylene Blue," *Acs Sustainable Chemistry & Engineering,* vol. 5, no. 10, pp. 8860-8869, 2017.

[5] G. Y. Zhu, T. Chen, Y. Hu, L. B. Ma, R. P. Chen, H. L. Lv*, et al.*, "Recycling PM2.5 carbon nanoparticles generated by diesel vehicles for supercapacitors and oxygen reduction reaction," *Nano Energy,* vol. 33, pp. 229-237, 2017.

[6] F. Liang, M. Lu, T. C. Keener, Z. Liu, and S.-J. Khang, "The organic composition of diesel particulate matter, diesel fuel and engine oil of a non-road diesel generator," *Journal of Environmental Monitoring,* vol. 7, no. 10, pp. 983-988, 2005.

[7] O. B. Popovicheva, C. Irimiea, Y. Carpentier, I. K. Ortega, E. D. Kireeva, N. K. Shonija*, et al.*, "Chemical Composition of Diesel/Biodiesel Particulate Exhaust by FTIR Spectroscopy and Mass Spectrometry: Impact of Fuel and Driving Cycle," *Aerosol and Air Quality Research,* vol. 17, no. 7, pp. 1717-1734, 2017.

[8] C. Walgraeve, K. Demeestere, J. Dewulf, R. Zimmermann, and H. Van Langenhove, "Oxygenated polycyclic aromatic hydrocarbons in atmospheric particulate matter: Molecular characterization and occurrence," *Atmospheric Environment,* vol. 44, no. 15, pp. 1831-1846, 2010.

[9] L. Turrio-Baldassarri, C. L. Battistelli, and A. L. Iamiceli, "Evaluation of the efficiency of extraction of PAHs from diesel particulate matter with pressurized solvents," *Analytical and Bioanalytical Chemistry,* vol. 375, no. 4, pp. 589-595, 2003.

[10] C. A. Alves, A. M. P. Vicente, J. Gomes, T. Nunes, M. Duarte, and B. A. M. Bandowe, "Polycyclic aromatic hydrocarbons (PAHs) and their derivatives (oxygenated-PAHs, nitrated-PAHs and azaarenes) in size-fractionated particles emitted in an urban road tunnel," *Atmospheric Research,* vol. 180, pp. 128-137, 2016.

[11] S. Decesari, M. C. Facchini, E. Matta, M. Mircea, S. Fuzzi, A. R. Chughtai*, et al.*, "Water soluble organic compounds formed by oxidation of soot," *Atmospheric Environment,* vol. 36, no. 11, pp. 1827-1832, 2002.

[12] K. Alena, S. T. S., G. J. R., H. S. B., and P. M. J., "Toxicity of wide-range polarity fractions from wood smoke and diesel exhaust particulate obtained using hot pressurized water," *Environmental Toxicology and Chemistry,* vol. 23, no. 9, pp. 2243-2250, 2004.

[13] F. L. Dickert, H. Besenböck, and M. Tortschanoff, "Molecular Imprinting Through van der Waals Interactions: Fluorescence Detection of PAHs in Water," *Advanced Materials,* vol. 10, no. 2, pp. 149-151, 1998.

[14] J. Zhang, Y. Fu, M. H. Chowdhury, and J. R. Lakowicz, "Metal-Enhanced Single-Molecule Fluorescence on Silver Particle Monomer and Dimer: Coupling Effect between Metal Particles," *Nano Letters,* vol. 7, no. 7, pp. 2101-2107, 2007.

[15] P. P. Pompa, L. Martiradonna, A. D. Torre, F. D. Sala, L. Manna, M. De Vittorio*, et al.*, "Metal-enhanced fluorescence of colloidal nanocrystals with nanoscale control," *Nature Nanotechnology,* vol. 1, p. 126, 2006.

[16] H. Ditlbacher, J. R. Krenn, N. Felidj, B. Lamprecht, G. Schider, M. Salerno*, et al.*, "Fluorescence imaging of surface plasmon fields," *Applied Physics Letters,* vol. 80, no. 3, pp. 404-406, 2002.

[17] K. Aslan, I. Gryczynski, J. Malicka, E. Matveeva, J. R. Lakowicz, and C. D. Geddes, "Metal-enhanced fluorescence: an emerging tool in biotechnology," *Current Opinion in Biotechnology,* vol. 16, no. 1, pp. 55-62, 2005.

[18] K. Aslan, J. R. Lakowicz, and C. D. Geddes, "Metal-enhanced fluorescence using anisotropic silver nanostructures: critical progress to date," *Analytical and bioanalytical chemistry,* vol. 382, no. 4, pp. 926-933, 2005.

[19] S. Rajeshkumar and L. V. Bharath, "Mechanism of plant-mediated synthesis of silver nanoparticles - A review on biomolecules involved, characterisation and antibacterial activity," *Chemico-Biological Interactions,* vol. 273, pp. 219-227, 2017.

[20] I. M. Chung, I. Park, K. Seung-Hyun, M. Thiruvengadam, and G. Rajakumar, "Plant-Mediated Synthesis of Silver Nanoparticles: Their Characteristic Properties and Therapeutic Applications," *Nanoscale Research Letters,* vol. 11, p. 14, 2016.

[21] U. B. Jagtap and V. A. Bapat, "Green synthesis of silver nanoparticles using Artocarpus heterophyllus Lam. seed extract and its antibacterial activity," *Industrial Crops and Products,* vol. 46, pp. 132-137, 2013.

[22] H. P. Borase, B. K. Salunke, R. B. Salunkhe, C. D. Patil, J. E. Hallsworth, B. S. Kim, *et al.*, "Plant Extract: A Promising Biomatrix for Ecofriendly, Controlled Synthesis of Silver Nanoparticles," *Applied Biochemistry and Biotechnology,* vol. 173, no. 1, pp. 1-29, 2014.

[23] A. M. El Badawy, K. G. Scheckel, M. Suidan, and T. Tolaymat, "The impact of stabilization mechanism on the aggregation kinetics of silver nanoparticles," *Science of The Total Environment,* vol. 429, pp. 325-331, 2012.

[24] A. R. Studart, E. Amstad, and L. J. Gauckler, "Colloidal Stabilization of Nanoparticles in Concentrated Suspensions," *Langmuir,* vol. 23, no. 3, pp. 1081-1090, 2007.

[25] C. Lourenco, M. Teixeira, S. Simões, and R. Gaspar, "Steric stabilization of nanoparticles: Size and surface properties," *International Journal of Pharmaceutics,* vol. 138, no. 1, pp. 1-12, 1996.

[26] H. Jiang, S. Manolache, A. C. L. Wong, and F. S. Denes, "Plasma-enhanced deposition of silver nanoparticles onto polymer and metal surfaces for the generation of antimicrobial characteristics," *Journal of Applied Polymer Science,* vol. 93, no. 3, pp. 1411-1422, 2004.

[27] K. Chaiseeda, S. Nishimura, and K. Ebitani, "Gold Nanoparticles Supported on Alumina as a Catalyst for Surface Plasmon-Enhanced Selective Reductions of Nitrobenzene," *ACS Omega,* vol. 2, no. 10, pp. 7066-7070, 2017.

[28] Y. Junejo, Sirajuddin, A. Baykal, M. Safdar, and A. Balouch, "A novel green synthesis and characterization of Ag NPs with its ultra-rapid catalytic reduction of methyl green dye," *Applied Surface Science,* vol. 290, pp. 499-503, 2014.

[29] R. M. Tripathi, N. Kumar, A. Shrivastav, P. Singh, and B. R. Shrivastav, "Catalytic activity of biogenic silver nanoparticles synthesized by Ficus panda leaf extract," *Journal of Molecular Catalysis B: Enzymatic,* vol. 96, pp. 75-80, 2013.

[30] R. Zhou and M. P. Srinivasan, "Photocatalysis in a packed bed: Degradation of organic dyes by immobilized silver nanoparticles," *Journal of Environmental Chemical Engineering,* vol. 3, no. 2, pp. 609-616, 2015.

[31] M. A. Garcia, "Surface plasmons in metallic nanoparticles: fundamentals and applications," *Journal of Physics D: Applied Physics,* vol. 44, no. 28, p. 283001, 2011.

[32] J. Tashkhourian, M. R. Hormozi-Nezhad, and M. Fotovat, "Optical Detection of Some Hydrazine Compounds Based on the Surface Plasmon Resonance Band of Silver Nanoparticles," *Spectroscopy Letters,* vol. 46, no. 1, pp. 73-80, 2013.

[33] M. M. K. Peiris, S. S. N. Fernando, P. M. Jayaweera, N. D. H. Arachchi, and T. D. C. P. Guansekara, "Comparison of Antimicrobial Properties of Silver Nanoparticles Synthesized from Selected Bacteria," *Indian Journal of Microbiology,* vol. 58, no.3, pp. 301-311, 2018.

[34] H. M. Esfanddarani, A. A. Kajani, and A. K. Bordbar, "Green synthesis of silver nanoparticles using flower extract of Malva sylvestris and investigation of their antibacterial activity," *Iet Nanobiotechnology,* vol. 12, no. 4, pp. 412-416, 2018.

[35] O. B. Popovicheva, C. Irimiea, Y. Carpentier, I. K. Ortega, E. D. Kireeva, N. K. Shonija, *et al.*, "Chemical Composition of Diesel/Biodiesel Particulate Exhaust by FTIR Spectroscopy and Mass Spectrometry: Impact of Fuel and Driving Cycle," *Aerosol and Air Quality Research,* vol. 17, no. 7, pp. 1717-1734, 2017.

[36] N. Ahmad, S. Sharma, V. N. Singh, S. F. Shamsi, A. Fatma, and B. R. Mehta, "Biosynthesis of Silver Nanoparticles from Desmodium triflorum: A Novel Approach Towards Weed Utilization," *Biotechnology Research International,* vol. 2011, p. 8, 2011.

[37] S. S. Shankar, A. Rai, A. Ahmad, and M. Sastry, "Rapid synthesis of Au, Ag, and bimetallic Au core–Ag shell nanoparticles using Neem (Azadirachta indica) leaf broth," *Journal of Colloid and Interface Science,* vol. 275, no. 2, pp. 496-502, 2004.

[38] H. M. M. Ibrahim, "Green synthesis and characterization of silver nanoparticles using banana peel extract and their antimicrobial activity against representative microorganisms," *Journal of Radiation Research and Applied Sciences,* vol. 8, no. 3, pp. 265-275, 2015.

[39] K. Yoosaf, B. I. Ipe, C. H. Suresh, and K. G. Thomas, "In Situ Synthesis of Metal Nanoparticles and Selective Naked-Eye Detection of Lead Ions from Aqueous Media," *The Journal of Physical Chemistry C,* vol. 111, no. 34, pp. 12839-12847, 2007.

[40] T. Schmitz, D. Hassel, and F.-J. Weber, "Determination of VOC-components in the exhaust of gasoline and diesel passenger cars," *Atmospheric Environment,* vol. 34, no. 27, pp. 4639-4647, 2000.

[41] M. J. O'Connell, C. K. Chan, W. Li, R. K. Hicks, S. K. Doorn, and H.-L. Wang, "Polyelectrolyte platform for sensitive detection of biological analytes via reversible fluorescence quenching," *Polymer,* vol. 48, no. 26, pp. 7582-7589, 2007.

[42] T. C. Dakal, A. Kumar, R. S. Majumdar, and V. Yadav, "Mechanistic Basis of Antimicrobial Actions of Silver Nanoparticles," *Frontiers in Microbiology,* vol. 7, no. 1831, 2016.

[43] Q. Feng, J. L. Wu, G.-Q. Chen, F.-Z. Cui, T. N. Kim, and J. O. A. Kim, "A Mechanistic Study of the Antibacterial Effect of Silver Ions on Escherichia Coli and Staphylococcus Aureus", *Journal of Biomedical Materials Research*, vol. 52, no.4, pp. 662-668, 2000.

[44] E. Fröhlich, "The role of surface charge in cellular uptake and cytotoxicity of medical nanoparticles," *International Journal of Nanomedicine,* vol. 7, pp. 5577-5591, 2012.

[45] M. K. Peiris, C. P. Gunasekara, P. M. Jayaweera, N. D. Arachchi, and N. Fernando, "Biosynthesized silver nanoparticles: are they effective antimicrobials?," *Memórias do Instituto Oswaldo Cruz,* vol. 112, pp. 537-543, 2017.

[46] K.-J. Kim, W. S. Sung, B. K. Suh, S.-K. Moon, J.-S. Choi, J. G. Kim, *et al.*, "Antifungal activity and mode of action of silver nano-particles on Candida albicans," *BioMetals,* vol. 22, no. 2, pp. 235-242, 2009.

[47] S. Sarina, E. R. Waclawik, and H. Zhu, "Photocatalysis on supported gold and silver nanoparticles under ultraviolet and visible light irradiation," *Green Chemistry,* vol. 15, no. 7, pp. 1814-1833, 2013.

AUTHORS

First Author- Dr. L. Palliyaguru, PhD, Senior Lecturer, Department of Chemistry, University of Sri Jayewardenepura, Palliyaguru@sjp.ac.lk.

Second Author – M.U.S. Kulatunga, MSc, Department of Chemistry, University of Sri Jayewardenepura, usameera11@gmail.com.

Third Author –Dr. K.G.U.R. Kumarasinghe, PhD, Senior Lecturer, Department of Chemistry, University of Sri Jayewardenepura, upulk@sjp.ac.lk.

Correspondence Author – Prof. P.M. Jayaweera, PhD, Senior Professor, Department of Chemistry, University of Sri Jayewardenepura, pradeep@sjp.ac.lk, +94714310805.